Combining bio-optical glider observations and biogeochemical modeling to examine potential Ross Sea phytoplankton changes in the 21st century

Daniel E. Kaufman*[1], Marjorie A. M. Friedrichs[1], Walker O. Smith Jr[1], Eileen E. Hofmann[2], Michael S. Dinniman[2], John C. P. Hemmings[3]

[1]Virginia Institute of Marine Science, College of William & Mary, [2]Center for Coastal Physical Oceanography, Old Dominion University, [3]Met Office, Exeter, UK

******For more info, please contact: dekaufman@vims.edu*

INTRODUCTION

The Ross Sea, a highly productive coastal bay of Antarctica, is dominated by the phytoplankton *Phaeocystis antarctica* and diatoms (Kaufman et al. 2014).

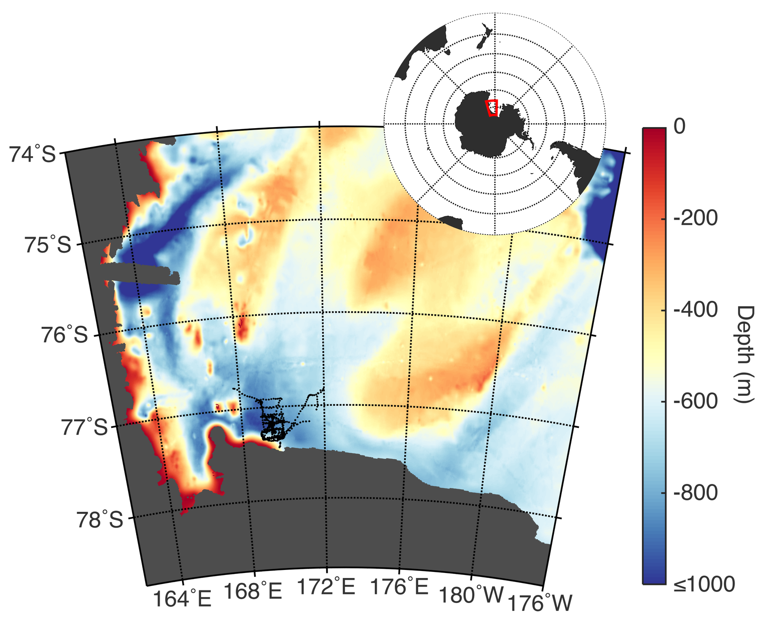

Figure 1: Southwestern Ross Sea showing the glider transect, overlaid on bathymetry of the shelf. Dark gray areas represent topography above sea level or glacial ice.

In the Ross Sea, projected climate-induced physical changes over the next century include (Smith et al. 2014):

- increased summer mixed layer temperatures,
- shallower mean mixed layer depths (MLDs),
- earlier melting of sea ice.

Research Question:

How will phytoplankton productivity and carbon export in the Ross Sea be affected by future climate-induced changes in temperature, mixing, and sea ice?

- Phytoplankton growth begins early each austral spring (late October) when *P. antarctica* grows rapidly and reaches maximum biomass in mid- to late-December (Smith et al. 2000).
- Growth and biomass of *P. antarctica* decline through January, and there is often a secondary bloom of diatoms (Peloquin and Smith, 2007).

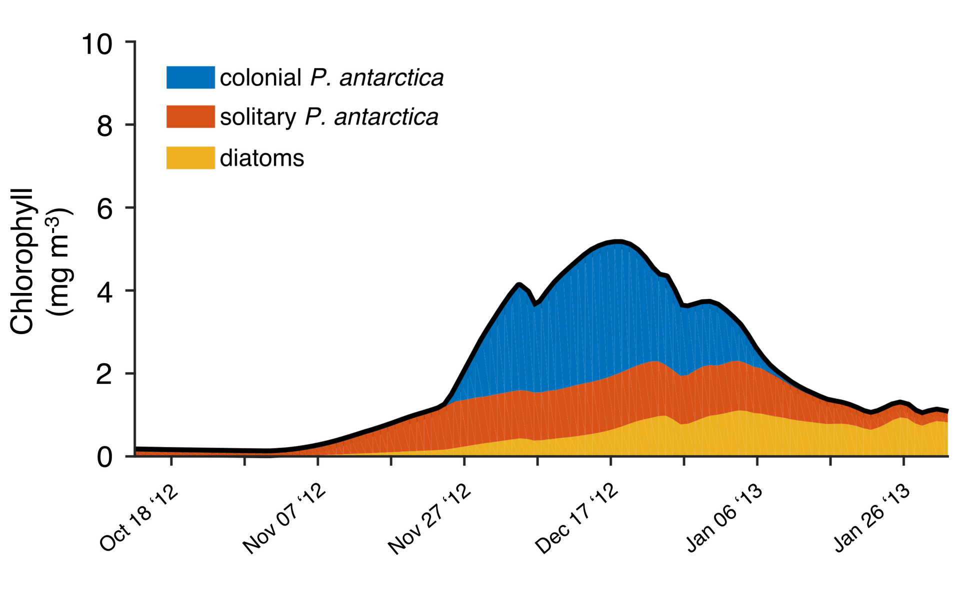

Figure 2: Time series of modeled chlorophyll for each phytoplankton group averaged over the upper 50 m.

METHODS

Model

The Model of Ecosystem Dynamics, nutrient Utilisation, Sequestration and Acidification was adapted for the Ross Sea (MEDUSA-RS) to include both solitary and colonial *P. antarctica* as well as diatoms (Kaufman et al. 2017a).

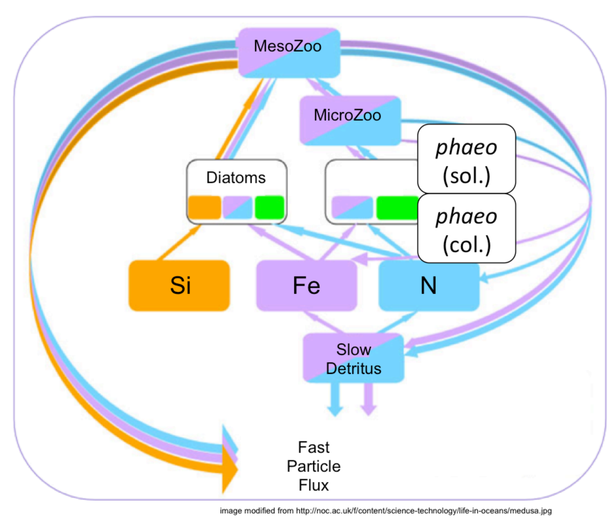

Figure 3: Model schematic showing the components of MEDUSA-RS, modified from Yool et al. (2011). MEDUSA-RS was run within MarMOT, a 1D model analysis framework (Hemmings et al. 2015) and contemporary simulations spanned Oct. 2012 to Feb. 2013 due to available glider data for this period.

Data

- Physical forcings were generated from glider measurements and other available dataset.
- Boundary conditions at 200m were set to climatological means for nitrate and silicate, and means of available data for dissolved iron (Kaufman et al. 2017b).

Figure 4: (below) An image of a Seaglider.

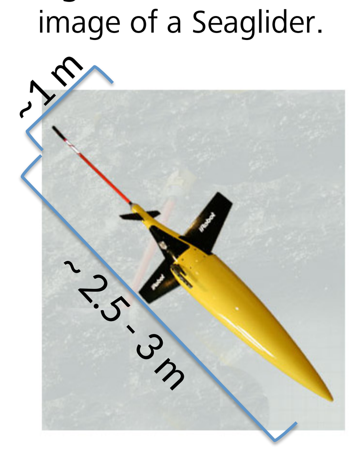

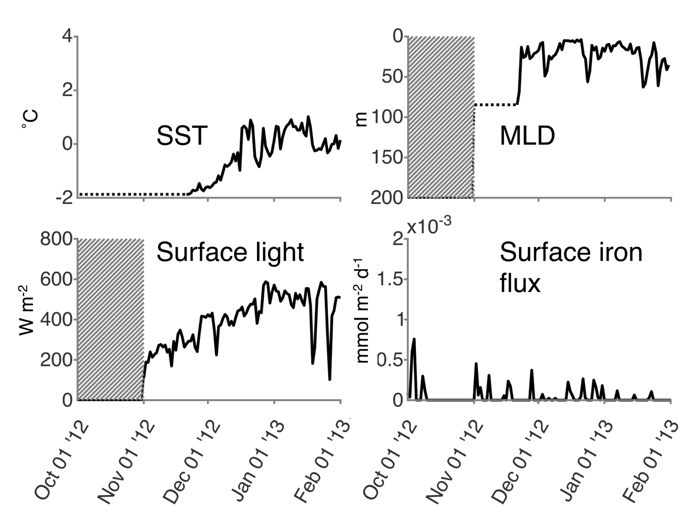

Figure 5: (above right) Model forcings include glider-derived temperature and MLD, irradiance attenuated by ice cover, and iron released into the surface layer as sea ice decreases. Hatched areas indicate times before ice melts in the model.

Contemporary Simulation & Assimilation

Chlorophyll and particulate organic carbon (POC) from the glider were assimilated into the model using MarMOT, and modeled distributions compared well with the observations (Kaufman et al. 2017c).

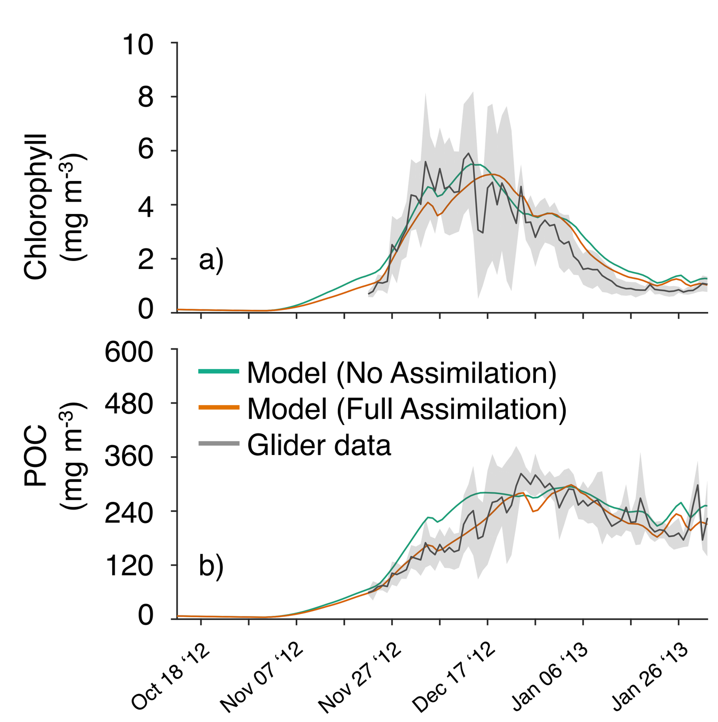

Figure 6: Mean modeled biomass from the contemporary simulation tuned by hand (green line), optimal simulation when assimilating the glider observations (orange line), and the glider data (black line) over the upper 50 m for (a) chlorophyll and (b) total POC, with shaded areas representing one standard deviation.

Climate Scenarios

Scenario experiments with MEDUSA-RS examined the response of phytoplankton to projected physical conditions (Table 1).

	2050	2100
Increased Temperatures	0.3 °C	0.8 °C
Shallower MLDs	6 %	29 %
Earlier Melting of Sea Ice	5 days	11 days

Table 1 (above): Simulations with a Ross Sea implementation of the Regional Ocean Modeling System (ROMS) were conducted to quantify projected physical changes for 2050 and 2100 for this area.

RESULTS

Primary productivity and carbon export are greater in both mid- and late-century scenarios compared to the contemporary estimate

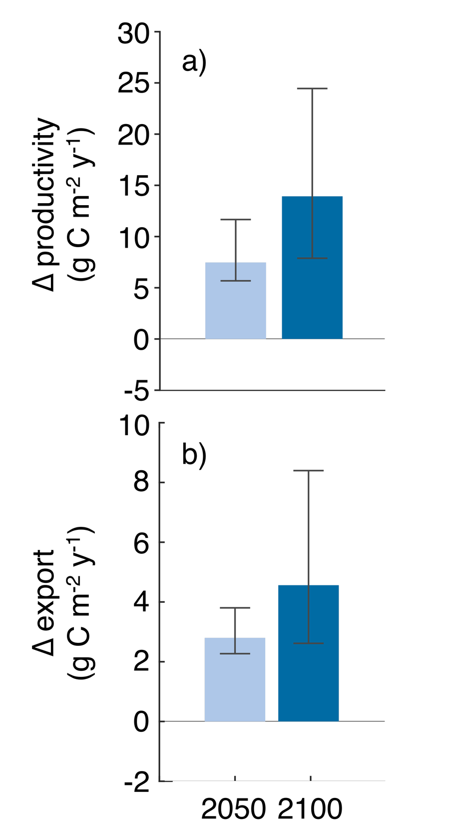

Figure 7 (left): Change in (a) productivity and (b) carbon export flux at 200 m from the contemporary control to the mid- and late-21st century climate scenarios. The effect of halving and doubling physical forcing deltas are shown by the capped error-bars.

Primary Productivity Increases 7-14%

Carbon export flux also increases, remaining ~26% of primary productivity

Earlier availability of light from melting sea ice is the primary driver of increased productivity in both mid- and late-21st century scenarios

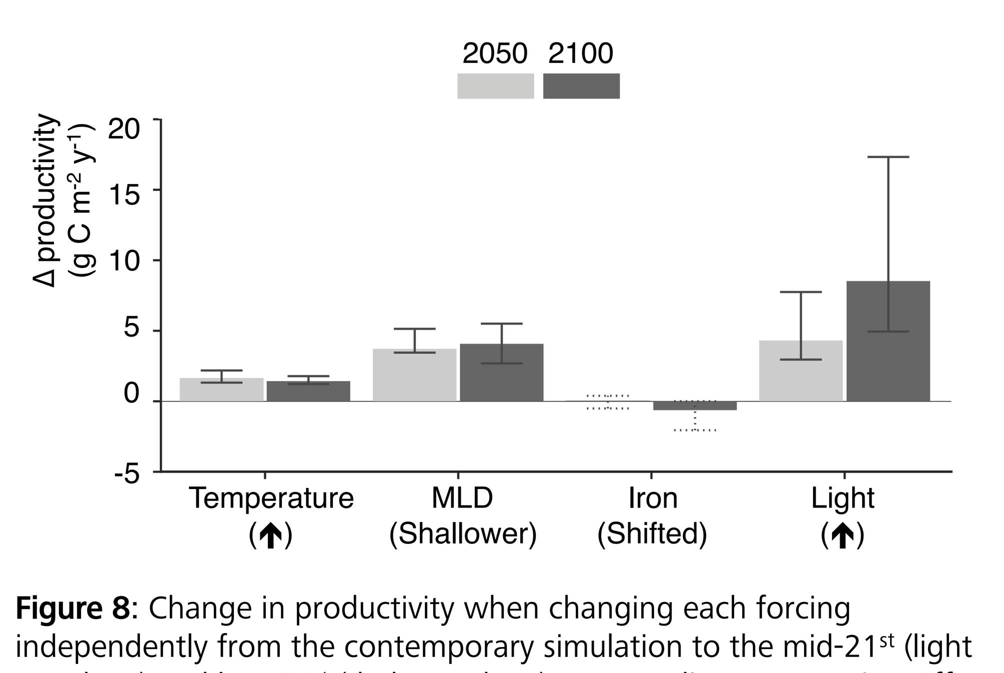

Figure 8: Change in productivity when changing each forcing independently from the contemporary simulation to the mid-21st (light gray bars) and late-21st (dark gray bars) century climate scenarios. Effects of halving and doubling physical forcing deltas (between contemporary and future scenarios) are shown by the capped error bars.

Shallower mixed layer depths cause diatom carbon to increase and Phaeocystis antarctica to decrease by the mid-21st century

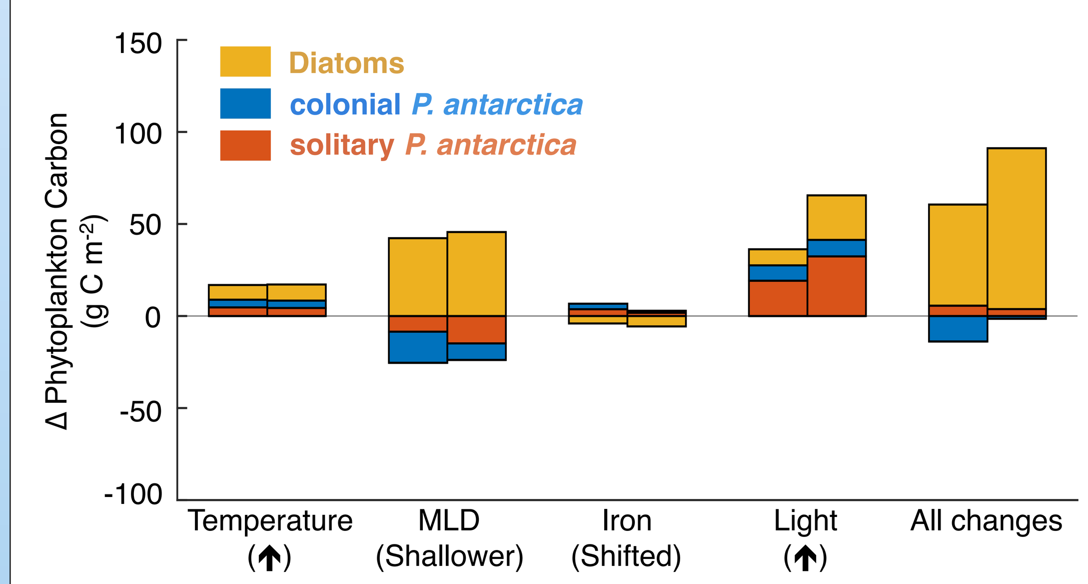

Figure 9: Changes in biomass of each phytoplankton group are shown between the contemporary simulation and the mid-21st (left bar in each pair) and late-21st (right bar in each pair) century climate scenarios. The left four pairs of bars show the effects of changing each forcing independently.

In midcentury the effects of irradiance changes are mitigated by MLD changes, whereas in the late-century scenario earlier melting of sea ice extends the growing season of *P. antarctica* into a period of lower average irradiances.

CONCLUSIONS

- Climate model scenarios for the mid-21st and late-21st century indicate increases of primary productivity and carbon export flux.
- Increased production over the next century is primarily driven by increased light availability as a result of melting sea ice. Other changes (temperature and changes in surface iron input) produce minor independent effects.
- Combined light and MLD changes modify the phytoplankton assemblage composition over the next century. Until 2050, increased production is largely a result of increased diatom production as they outcompete *P. antarctica* under higher light conditions. By 2100, availability of low light early in the season allows productivity of *P. antarctica* to rebound to its contemporary level.

Acknowledgments

This work was funded in part by the National Science Foundation's Office of Polar Programs (NSF- ANT-0838980, PIs W. Smith, M. Friedrichs, and E. Hofmann).

References

Hemmings, J.C.P., et al. (2015) G.M.D. 8, 697–731.
Kaufman, D.E., et al. (2014) D.S.R. I 92, 93–106.
Kaufman, D.E., et al. (2017a) J.G.R.-O., 122, 2339-2359.
Kaufman, D.E., et al. (2017b) W&M Publish, doi: 10.21220/V5PC71
Kaufman, D.E., et al. (2017c) B.G., In review.
Peloquin, J.A. and Smith, W.O., et al. (2007) J.G.R., 112, 1-12.
Smith, W.O., et al. (2000) D.S.R. II 47, 3119–3140.
Smith, W.O., et al. (2014) G.R.L. 41, 1624–1631.
Yool, A., et al. (2011) G.M.D. 4, 381–417.